Analytica Chimica Acta 1229 (2022) 340345

Contents lists available at ScienceDirect

Analytica Chimica Acta

journal homepage: www.elsevier.com/locate/aca

Geometric characterization of polymeric capillaries

Enas N. Yousef [a], Purnendu K. Dasgupta [a,*], Seth A. Horn [a], C. Phillip Shelor [a], Souvik Roy [b]

[a] Department of Chemistry and Biochemistry, University of Texas at Arlington, Arlington, TX, 76019-0065, United States
[b] Department of Mathematics, University of Texas at Arlington, Arlington, TX, 76019-0408, United States

HIGHLIGHTS

- Multiple methods, most used for the first time were compared for measuring the i. d. of small-bore capillaries.
- Different approaches produce concordant results for uniform bore capillaries.
- A quantitative index for concentricity is defined for the first time.
- Different diameter dependence of two measurement techniques permits the determination of both true diameter and its variance.
- OT column theory suggests that chromatographic performance is dependent only on the mean diameter and not on its variance.

GRAPHICAL ABSTRACT

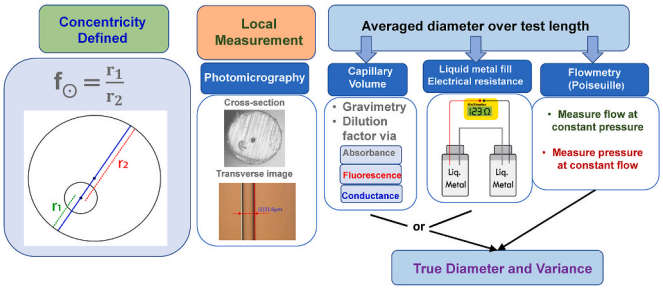

ARTICLE INFO

Keywords:
Capillary diameter
Open tubular liquid chromatography
Bore uniformity
Circularity
Concentricity

ABSTRACT

There are few methods in the literature to measure the inner diameter of very small capillaries. Although silica capillaries are more commonly used, synthetic polymer capillaries are preferred in some applications. The technology for producing them is not as mature. Aside from the absolute value of the inner diameter, the circularity, concentricity (a quantitative index is defined here for the first time) and the bore uniformity of such capillaries are of interest. Beyond microscopy, we describe multiple methods that determine the capillary inner diameter, averaged over a given length. The measurements variously depended on the capillary internal volume, length and cross section, and the resistance to fluid flow. The different approaches produced mutually consistent results. We show that when the internal diameter is not uniform, the different dependence on diameter that two such methods may exhibit, can be exploited to determine the true mean diameter as well as its variance. Finally, for open tubular liquid chromatography, where performance acutely depends on the inner diameter, we surprisingly find that while the mean i.d. may be the dominant determinant of efficiency, bore variance has little to no effect on the performance.

1. Introduction

The invention of the glass capillary drawing machine by Desty et al., in 1960 [1] was a major milestone in analytical sciences, specifically in gas chromatography. Open tubular liquid chromatography (OTLC) was shortly introduced by Nota et al., in 1970 [2]. It was almost another decade later that Dandeneau and Zerenner pointed out and demonstrated the vast superiority of fused silica over soda- or borosilicate glass

* Corresponding author.
E-mail address: Dasgupta@uta.edu (P.K. Dasgupta).

https://doi.org/10.1016/j.aca.2022.340345
Received 27 June 2022; Received in revised form 29 August 2022; Accepted 1 September 2022
Available online 13 September 2022

[3]. Many areas of analytical science would be hard to imagine today without fused silica capillaries. Fused Silica has several unique properties, ranging from its optical transparency over broad wavelength ranges to its superb mechanical strength. A large range of chemistries have been developed to etch and functionalize silica surfaces. Still, it is not without a few shortcomings in certain specific applications. Most strategies to functionalize silica cannot produce linkages stable in strong base. Indeed, silica itself dissolves in strong base. Huang and Horváth [4] went to the trouble of polymerizing a thin sheath of styrene-divinylbenzene inside a silica capillary to circumvent this. Second, while the rigidity of silica makes for high pressure tolerance, there are stringent limits to how tightly a silica capillary can be coiled, even with protective sheathing. In a straight or large radius-of-curvature tube, mass transfer to the walls of the tube is governed by diffusion alone. In contrast, for tubes that are coiled into a small diameter, centrifugal flow can be harnessed to become an added vector for enhancing transport to the wall [5–8], of considerable import and benefit to open tubular chromatographic (OTC) separations.

We are particularly interested in OT ion exchange separations, which began in the early 80's with the work of Ishii and Takeuchi [9]. They used 30–60 μm φ (used hereinafter to denote inner or bore diameter, these terms are used interchangeably) glass capillaries, functionalized with a suitable silane and subsequently further reacted to provide $–SO_3H$ groups for cation exchange sites to separate protonated nucleosides followed by detection via optical absorption. They reported cation exchange capacities of ~12 peq/mm^2 (where peq denotes picoequivalent; note that it is numerically the same as μmol/m^2), essentially corresponding to a monolayer coverage of the smooth glass surface. In open tubular liquid chromatography, increase in capacity is always desirable. They were able to increase the capacity by an order of magnitude by prior NaOH etching of the glass. Hydrothermal processes do this even more effectively [10].

Going to smaller bore diameters not only increases separation efficiency, the increase in surface to volume ratio is also tantamount to an increase in relative capacity. But sensitive detection has always been a problem. Beginning in 1983 and continuing till 1991, Simon's group published a series of pioneering papers [11–13] on Open Tubular Ion Chromatography (OTIC) centered on their extremely small volume (~1 μm tip) ion-selective microelectrode based potentiometric detector and fused silica columns 2.3–25 μm φ. Such remarkable early achievements impressed and inspired many, including the senior author of this paper. But his early hopes of doing such separations in polymeric capillaries were dashed: attempts at getting small bore polystyrene capillaries extruded did not succeed in producing capillaries any smaller than 125 μm φ [14].

We thus started our journey in OTIC with 50 μm φ silica capillaries far later, in 1997. Positively charged latex particles were electrostatically attached to negatively charged silanol bearing walls, or dynamic wall coatings of cationic surfactants were used to generate anion exchange sites. Elevated temperatures (up to 100 °C) were used to enhance diffusive transport, but detection was limited to UV-absorbing analytes [15].

Since its inception to current practice, commercial practice of anion chromatography has utilized alkaline eluents. In the OT adaptation, we continued to try to use silica capillaries, much like others engaged in any type of capillary separations. The use of an alkaline eluent and full adaptation of macroscale IC to OTIC remained impractical. Masking silanol groups with other protective groups generally fails to make them compatible with high pH eluents [16]. However, a multilayer amine-epoxide stationary phase (up to 25 layers) [17] did permit the use of an alkali hydroxide eluent, at least for some period, but fabrication of such columns are very time consuming.

The technology of producing fused silica capillaries is presently highly refined. Down to 2 μm φ, capillaries are not only available as stock items; their utility in separations have been repeatedly demonstrated [18,19]. From better vendors, the circularity and concentricity of silica capillaries are near-perfect, such that even small capillaries can be butt-joined without issues [20]. Any significant length of such capillaries typically comes with beginning and ending i.d. and o.d. specified, which may provide some idea of the bore uniformity. (Note that the above statements are not universally true, we have purchased relatively inexpensive imported silica capillaries that display far from ideal geometry).

In 2012, we were able to have polymethylmethacrylate capillaries of suitable dimensions extruded, characterization [21] and chromatography [22] soon followed. Since then, we have had extruded capillaries of cyclic olefin polymer (COP), cyclic olefin copolymer (COC), polyetherimide (PEI, Ultem®), and high-density polyethylene (HDPE). In the interim, PEEK capillaries of nominally 25 μm φ have become commercially available. Attractive chromatographic performance has been observed with COP [23], PEEK [14] and HDPE capillaries (unpublished data). Unlike silica capillaries, however, the circularity, concentricity, and bore uniformity of most are far from ideal; some of the first two parameters so much so that the capillaries are unusable altogether. Also, unlike silica capillaries, no accurate reliable measure of the bore diameters (φ) of these capillaries is available *a priori*. In our experience, the actual inner diameter of commercial PEEK capillaries varies widely from the stated 25 μm, for example. In the next section we describe the importance of each of these parameters and their measurement.

2. Principles

2.1. Circularity

Circularity (f_o) is a shape metric of how closely the outer perimeter (P) of a tube describes a circle of cross-sectional area A; mathematically it is defined as [24].

$$f_o = \frac{4\pi A}{P^2} \tag{1}$$

For a perfect circle, f_o has the maximum possible value, unity. For comparison, a square and an equilateral triangle would have respective f_o values of 0.785 and 0.605. In chromatography, connecting fittings typically rely on a compression ferrule of circular cross section. If circularity is poor, when the ferrule is in contact with one side of the tube, it still does not contact some other section(s) of the tube perimeter. Therefore, to achieve a seal, excessive compression has to be applied, often resulting in complete closure of the central bore because this is the most collapsible region. Circularity was measured by imaging the cross section and using subroutines built into Image J for this specific measurement [24].

2.2. Concentricity

Concentricity of the separation tube is not important for the separation itself. But it is crucial in connecting the tube to the external world. The separation conduit is connected to the injector and detector at each end, typically mating with apertures of comparable bore. It is not uncommon, for example, for the separation column to be butt-joined to another tube that serves as the electrospray emitter acting as the ion source for a mass spectrometric detector [25]. A similar situation exists at the injector end. If the bores are not concentric, they will not line up with the injector aperture, creating a major restriction and may shut off flow altogether. The challenge of mating is better understood when one considers that for a 365 μm dia. capillary of 20 μm φ, the bore area represents only 0.30% of the cross-section!

We were unable to find a quantitative definition of concentricity in the literature. Of course, the concept of concentricity is only meaningful if the tube cross section as well as the inner bore have sufficiently high circularity such that a center can be defined in both cases. Perfect concentricity in a tube is then easily seen as the situation when the outer perimeter (tube as a whole) and the inner bore (the channel) share the

same center. We define the concentricity metric ($f_{\odot}$) as

$$f_{\odot} = \frac{r_1}{r_2} \tag{2}$$

where, referring to Fig. 1, r_1 and r_2 are respectively the two distances from the bore to the perimeter along the line joining the two centers, r_1 being $\leq r_2$. Obviously, the two centers are the same for a perfectly concentric tube. This definition leads to a similar quantitative index as in f_o, the maximum value of $f_{\odot}$ is unity as well. Other metrics of concentricity can be concieved but it seems that the present one is the simplest, the most straightforward and the most generally applicable. Occasionally, one may be interested in capillaries that do not have a circular perimeter or the bore is not perfectly circular. In such cases we suggest concentricity (or circularity) be computed by fully enclosing such an irregular perimeter (of the tube or the bore) by a circle of the smallest possible diameter.

We measure $f_{\odot}$ by photomicrographically imaging the cross section. The requisite measurements are provided by the microscope software.

3. Diameter measurement strategies

The literature on the measurement of capillary diameters is scant. With one exception [26], the extant studies were mostly based on various forms of microscopy and centered on the measurement of diameters of biological capillaries, typically carried out by staining and microscopic examination [27,28] and occasionally by digital scanning laser fluorescence angiography [29].

3.1. Photomicrographic imaging

Photomicrographic imaging of the cross section, processed by image analysis software, is an obvious approach if equipment of sufficient resolution is available. For capillaries that are transparent or translucent (such as those of PMMA, PEI, COP, HDPE, silica, etc.) transverse imaging of the bore is also possible. This in turn permits nondestructive imaging at multiple locations from which the bore uniformity can be ascertained. However, as the inner edge of the bore is largely determined by contrast, the perceived edge location is affected by the refractive index of the fill fluid. The curved surface also affects the absolute accuracy of such a measurement.

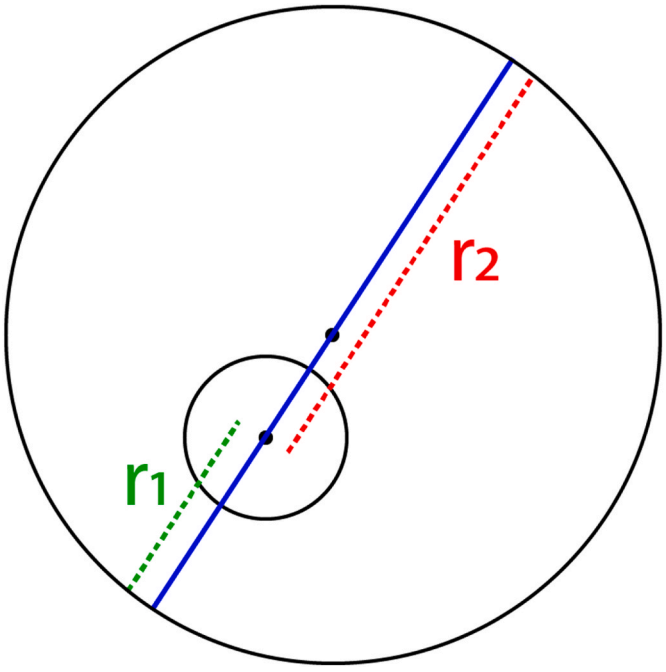

Fig. 1. Illustrative cross section of a capillary with a substantially non-concentric bore. The • marks depict the center of the bore and the center of the outer perimeter. The solid line joins the two centers. r_1 and r_2 respectively defines the distance of the bore center to the opposite sides of the perimeter, r_2 being greater (or equal) than (to) r_1.

3.2. Via measurement of capillary volume

The measurement of the volume V of liquid contained in a specific known length L of a capillary can be used to ascertain the bore φ of a capillary from

$$\varphi = 2\sqrt{\frac{V}{\pi L}} \tag{3}$$

The volume in turn can be measured in two principal ways.

3.2.1. Gravimetry

This involves measuring the weight of a known length (L) of an air-filled capillary (W_1) and then reweighing it after filling with a liquid (e.g., water, mercury, etc., of density ρ). The diameter can then be obtained from

$$\varphi = 2\sqrt{\frac{(W_2 - W_1)}{\pi \rho L}} \tag{4}$$

As an analytical balance is likely the instrument with the greatest absolute accuracy in any laboratory, as long as the weight difference is sufficient for the resolution of the balance, uncertainty in weighing is not likely to be a significant factor in the overall uncertainty. Similarly, the density of a common pure liquid is likely to be known with relatively high accuracy. While the length itself can be relatively accurately measured, the largest error is likely to originate from uncertainties in the degree to which the tube can be exactly filled. The method allows for multiple measurements with different tube lengths, the relative fill-error decreases with increasing length.

3.2.2. Dilution factor measurement

If the capillary tube of volume V is filled with the solution of a highly colored or fluorescent dye or a highly conducting electrolyte of known concentration (C_{known}) and the contents are expelled and diluted to a known volume (V_{dil}), the diluted concentration (C_{dil}) can be determined using a calibration plot of absorbance/fluorescence/conductance vs. concentration that is constructed centered around C_{dil}. The tube diameter is then computed from:

$$\varphi = 2\sqrt{\frac{C_{dil} V_{dil}}{\pi L C_{known}}} \tag{5}$$

The largest uncertainty in this case is contributed again by exactness of filling of the capillary, to which is now added the completeness of the expulsion of the filled solution.

3.3. Direct conductometry (measurement of the resistance of the capillary filled with a conducting fluid)

Measuring the electrical resistance of the tube filled with a conductive liquid (of known specific resistivity ψ) was first suggested by Guthrie et al. [26] who measured the electrical resistance R of a mercury-filled glass capillary placed between two mercury-filled reservoirs. The capillary diameter is then given by:

$$\varphi = 2\sqrt{\frac{\psi L}{\pi R}} \tag{6}$$

Different tube lengths can be used to check the uniformity of i.d. across different lengths. The method is simple and straightforward. If the purity of the mercury is uncertain, the system can be calibrated with one or more silica capillaries of known φ. However, the toxicity of mercury,

and therefore the precautions that must be taken to deal with this easily spilled liquid, are deterrents. As most electrical resistance measurement devices are quite accurate (even NIST traceable certified instruments are not prohibitively expensive) the errors will primarily come from measuring the length of the capillary and the assumed value of the electrical resistivity of mercury. It is not easy to replace a conducting metal in this application with an electrolyte solution as the resistance of the mercury column in a 1-m capillary of 20 μm φ is already in the kΩ range and even the most concentrated electrolyte solutions are ~4 orders of magnitude less conductive than mercury. Issues with replacing mercury by a less hazardous liquid metal/alloy such as that of Ga-In-Sn (e.g., Galinstan [30]) are discussed in the results section.

3.4. Using the Hagen-Poiseuille relationship

For a tube of a given length and a liquid of known viscosity, the Hagen-Poiseuille equation indicates that the pressure needed to achieve a certain flow rate increases with the fourth power of $\frac{1}{\varphi}$. The flow rate can be measured at various pressures using a pneumatic pump or HPLC equipment that allows delivering liquids at a constant known flow rate while the head pressure is read out. It is thus possible to measure the pressure drop ΔP at a known flow rate Q. The diameter is then calculated from

$$\varphi = \sqrt[4]{\frac{128\eta LQ}{\pi \Delta P}} \tag{7}$$

The opposite is also possible, to measure the flow rate from the exit end of the capillary while various known pressures are applied, e.g., from a pneumatically pressurized liquid reservoir. The liquid flow rate at the exit end can be measured by gravimetry or a nanoflow meter. Water would be the preferred liquid, as it is easily available in pure form, and its kinematic viscosity η is accurately known as a function of temperature. In the known constant flow rate experiment using an HPLC pump, under optimum conditions, the flow rate and pressure can be set/read with an accuracy of ≤1%. Such pumps do not work well in the absence of a significant back pressure, however. Additionally, there is always some flow restriction between the pressure transducer and the connection to the test capillary. It is necessary to first connect a flow restrictor, (e.g., a HPLC (guard) column, or a capillary restrictor) to the pump outlet to provide sufficient backpressure for proper operation. The test capillary is then connected after the restrictor. The pressure difference with and without the capillary connected is taken as ΔP. When compression fittings are used to connect the capillary, with soft polymer capillaries the compression seal may produce additional pressure drop in the connection that is not accounted for and will cause a negative error in the calculated φ. This effect can be compensated for by beginning with a long capillary and after the first measurement is done, cutting off a known length and measuring again. The process is then repeated. The slope of the pressure drop as a function of capillary length eliminates the influence of any additional pressure drop across any upstream components or restrictive connections.

In the constant pressure mode, the flow rate may be read with a nanoflow meter. These typically come with traceable certification of accuracy. However, such flow meters typically have a capillary flow channel within them, and the pressure drop due to the meter itself must first be measured before a capillary is connected downstream. In collecting effluent liquid and weighing, evaporation losses can cause errors but can be minimized by an appropriate strategy of collection and extending the collection time. With water used as the pumped liquid, and its amount being determined by weight, the relevant equation is:

$$\varphi = \sqrt[4]{\frac{128\eta LW}{\pi \Delta P \rho t}} \tag{8}$$

where W is the weight of the liquid of density ρ collected over time t.

For both approaches (constant flow and constant pressure) the calculation of the diameter involves taking the fourth root of the known or measured quantities and thus considerably reduces the uncertainty of the computed diameter.

4. Experimental

4.1. Chemicals

Galinstan was obtained from www.rotometals.com. All other chemicals are commonly used and were obtained from standard chemical suppliers.

4.2. Capillaries

Most measurements were made for the high density polyethylene (HDPE) capillaries, nominally 20 μm φ, 365 μm o.d. (custom extruded by www.zena-membranes.cz). Other capillaries measured included those made of PEEK (nominally 25 μm φ, 360 μm o.d.; P/N 1574, www.idex-hs.com), Polyetherimide (PEI, Ultem 1000®, custom extruded by www.microspecorporation.com), and fused silica (nominally 25 μm φ, 375 μm o.d., TSP025375 www.molex.com).

4.3. Photomicrographic measurements

Photomicrographic measurements were made with a Keyence VHX-5000 digital microscope (www.keyence.com). Measurement of circularity, concentricity and bore were performed using ImageJ (https://imagej.nih.gov/ij/).

Perpendicular burr-free cross sections can be obtained for PEEK capillaries using polymeric capillary cutters (e.g., A-350. Idex-hs.com) but HDPE capillaries often get deformed in the process. The best results we have obtained are by putting the tube in a guillotine-like holder and using a freshly opened carbon-steel scalpel blade. Cross sections were obtained randomly over a 40 cm length to judge uniformity.

4.4. Measurement of capillary volume

4.4.1. Gravimetry

An empty capillary was wrapped at each end with the smallest feasible amount of Parafilm M and weighed (Mettler AT261, 0.01 mg readability, 0.015 mg reproducibility). The Parafilm pieces were taken off and the capillary connected to a water-filled glass vial contained within a stainless steel (SS) column packing reservoir (www.nextadvance.com), with the tip dipping into the water and affixed in place with compression fittings but without overtightening (must be especially careful with the soft HDPE capillaries). Approximately 50–100 psi N_2 pressure (depending on the capillary length, 1 psi = 6.895 kPa) was applied to the reservoir to completely fill and wash the capillary. After shutting off the source pressure and venting the reservoir, excess water was blotted from the capillary tip and sealed with one of the Parafilm pieces. The other end was then carefully removed from the pump, blotted and sealed with the remaining parafilm piece, and the capillary carefully weighed again, with the length of any void at each end being carefully noted. Similar experiments were also done with Galinstan as the fill-fluid.

4.4.2. Dilution factor measurement

4.4.2.1. Via conductance. A bipolar pulse conductometer (CDM-1, Dionex corp.) calibrated with 1.00 mM KCl solution was used for measuring specific conductance. All solutions were aspirated by a peristaltic pump through the conductance measurement cell at ~0.2 mL/min and the conductance values were measured under flowing conditions. A 1.073 M KCl solution was used to fill 4 different lengths of

HDPE capillaries (25, 50, 75, 100 cm, each measured twice), in a manner similar to what was done in section 4.4.1 to fill a tube with water. After venting, the capillary in the reservoir was lifted above the solution surface and the KCl in the tube was pneumatically delivered to a 10-mL volumetric flask and made up to the mark. The conductance data were translated to concentration by calibration with standards in the relevant range (6.0–48.0 μM KCl).

4.4.2.2. Via absorbance. This experiment was conducted in the same fashion as the conductance measurement experiments except the fill solution was a ~67 mM solution of bromothymol blue that was prepared by adding just enough base to dissolve it. The tube contents were then delivered into a 10-mL volumetric flask and made up to volume with 10 mM HCl. The absorbance values of the diluted solutions were measured at 440 nm on an Agilent 8453 diode array spectrophotometer and interpreted using a calibration curve spanning 0.2–3.8 μM solution of the dye.

4.4.2.3. Via fluorescence. The experiment was conducted in the same fashion as the absorbance measurement experiments with the fill solution being 55.95 mM fluorescein. The contents were delivered into a 10-mL volumetric flask and made up to volume with 10 mM NaOH solution. The fluorescence of these diluted solutions were measured with a Hitachi-FL-F2710 spectrofluorometer with excitation at 475 nm (5 nm slit) and the emission in the 510–520 nm range was integrated. The concentrations of the diluted solutions were interpreted from a calibration plot based on 0.250–4.00 μM fluorescein in 10 mM NaOH.

4.5. Electrical resistance measurement

A small amount of mercury was put inside the column packing reservoir, directly without a vial, and a capillary of known length was inserted into the reservoir with the tip just dipping into the mercury and affixed in place. The reservoir itself serves as one electrical contact. Approximately 400–600 psi (depending on the capillary length) N_2 pressure was applied to the reservoir with the distal end of the capillary being put in a glass vial. When mercury started coming into the glass vial, more mercury was added to the vial to form a convenient electrical contact. The resistance was measured by a Fluke 77 meter calibrated in the desired range with a precision resistance box. Upon completion of the experiment, the mercury in the capillary was pneumatically expelled. The experiment was repeated with a capillary of a different length.

CAUTION: Mercury is easily spilled, and mercury vapor is neurotoxic. This experiment must be conducted in a hood with spill barriers and sulfur on hand to cover the mercury in case of a spill.

Experiments with Galinstan were carried out in a similar fashion except that it was contained in a plastic microvial inside the SS pressure reservoir and a U-shaped stiff Platinum coated Niobium wire (0.5 mm dia., anometproducts.com) one end dipping into the vial and the other end contacting the steel reservoir). The outside of the reservoir again served as one electrical contact. Direct contact of Galinstan with the steel reservoir was avoided as this material sticks to most surfaces. The other contact was a similar Pt-coated Nb-wire dipped into the receiving microvial.

4.6. Flowmetry at constant pressure and pressure measurement at constant flow

Both these experiments were performed with the same three 1-m lengths of HDPE capillaries (HDPE-1 through HDPE-3) using water in the pneumatically pressurized reservoir. For the constant pressure experiment, a calibrated digital pressure controller (Parker-Hannifin Precision Fluidics OEM-EP-990-005123-100, 100 psi FS) was used to apply a fixed pressure of 78.9 psi to the reservoir containing water and the flow rate was measured gravimetrically. In the constant flow experiment, a nanoflowmeter (Sensirion AG, LG16-0025D, 1.5 μL/min FS) was used to measure the exit flow (100, 500, 750, and 1000 nL/min) and a larger range digital pressure controller (GX1ANKKZP900PSG1, proportionair.com, 900 psi FS) was used to vary the pressure on the reservoir until the desired flow rate was obtained.

5. Results and discussion

5.1. Photomicrography

5.1.1. Cross section imaging for bore diameter, circularity and concentricity

Fig. 2 shows cross section images of a variety of capillaries. Circularity and concentricity of these particular cross sections are also listed. Fig. 3 shows three of the better polymeric capillaries. In each case, triplicate images are shown for cross sections from different portions of the tube, but each comes from the same manufacturing batch. For these specific sections examined, the relative standard deviations of φ range from 2.7%, 4.8%, and 17% for the PEEK, HDPE, and PEI capillaries. Five further randomly taken cross sections for the HDPE capillaries were examined to gauge the reliability of such measurements: these results averaged 20.4 ± 0.8 μm (see Table S1 in the supporting information), indistinguishable with the results in Fig. 3. Clearly, some of these capillaries (e.g., the PEI) exhibit more bore variation than the others. Further, the real diameter of the capillary can be quite different from the manufacturer stated φ value, For the PEEK capillary, it was 50% higher.

Concentricity varies widely among the tubes and good circularity does not assure good concentricity. One cannot help but note that the PEI capillaries have both the poorest uniformity and concentricity, however we do not have sufficient data to decide if this is a general occurrence and whether the two can be related.

5.1.2. Transverse imaging

Several of the capillaries are transparent/translucent and it is possible to get some idea of the bore uniformity by nondestructive transverse imaging. Fig. 4 illustrates transverse images of the same HDPE capillary filled with different fluids. The mean (±sd) and median φ values from non-optical measurements (see Table 1) were 21.6 (±1.2) and 21.0 μm, respectively. Based on these results, only the measurements in b, c and e fall in the 95% confidence interval and even e can be excluded at the 90% confidence level. Given these results, the absolute accuracy of transverse optical measurements should be considered suspect. One reason is optical distortion caused by the curvature of the tube that acts like a magnifying lens (also affected by the refractive index (RI) of the fill fluid). A silica capillary (cross section imaging gives φ 25.15 ± 0.2 μm) measures 31.6 μm air-filled in transverse imaging. Although this is a rather extreme example, the same φ measured >20% higher (38.1 μm) when filled with a very high RI liquid (diiodomethane, RI 1.74, Fig. 5).

In transverse imaging, the diameter is measured edge to edge, where the edge is determined not by the user, but by the imaging software. Regardless, it was of interest to further examine the extent of fill-liquid dependence and any observer dependence. Transverse observation of four locations of two separate 1-m segments of water or fluorescein-filled HDPE capillary averaged identical diameters (21.2_5 μm) with 2–5% RSDs by the same observer (See Figure S1 in the SI). Another 1-m segment of an air-filled HDPE capillary was examined by two separate observers (observer A, who did the two liquid-filled experiments above, and observer B, conversant with the equipment but who did not perform such diameter measurements routinely). The average diameter observed by observer A was 21.5 ± 2.1 μm, statistically indistinguishable from the liquid filled capillary observations but with substantially larger variance than the previous cases. Observer B's results averaged 18.2 ± 1.5 μm, statistically different at the 95% probability level with either liquid filled data but not from observer A's air-filled measurements due to the relatively large variances of both of these datasets.

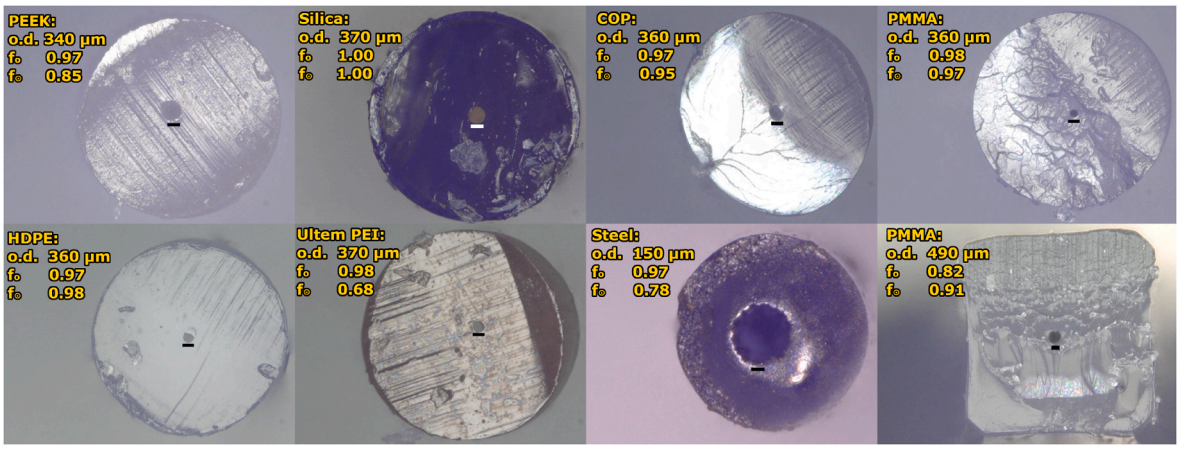

Fig. 2. Photomicrograph of cross sections of several capillaries. Only the silica and PEEK capillaries are available commercially, off the shelf. The circularity is perfect for the silica capillaries and very good to excellent for all the others as well, except of course for the square PMMA capillary; although if based on a circumscribed circle it will have a circularity of 0.97, indicating reasonable symmetry. As to concentricity, the silica capillaries again reach perfection. Those of the HDPE and PMMA capillaries are also very good; that for the COP capillary is acceptable. Concentricity of the PEEK and the stainless steel (note that this has a much smaller outer diameter) capillaries are poor and that for the PEI capillary is the worst among the set. Defined in terms of circumscribed circles (longest diagonal 490 µm), the concentricity of the square capillary is reasonable. Except for the steel capillary where the scale bar is 10 µm, all the other scale bars are 20 µm. PMMA is hard and brittle, and a smooth cross section is difficult to obtain.

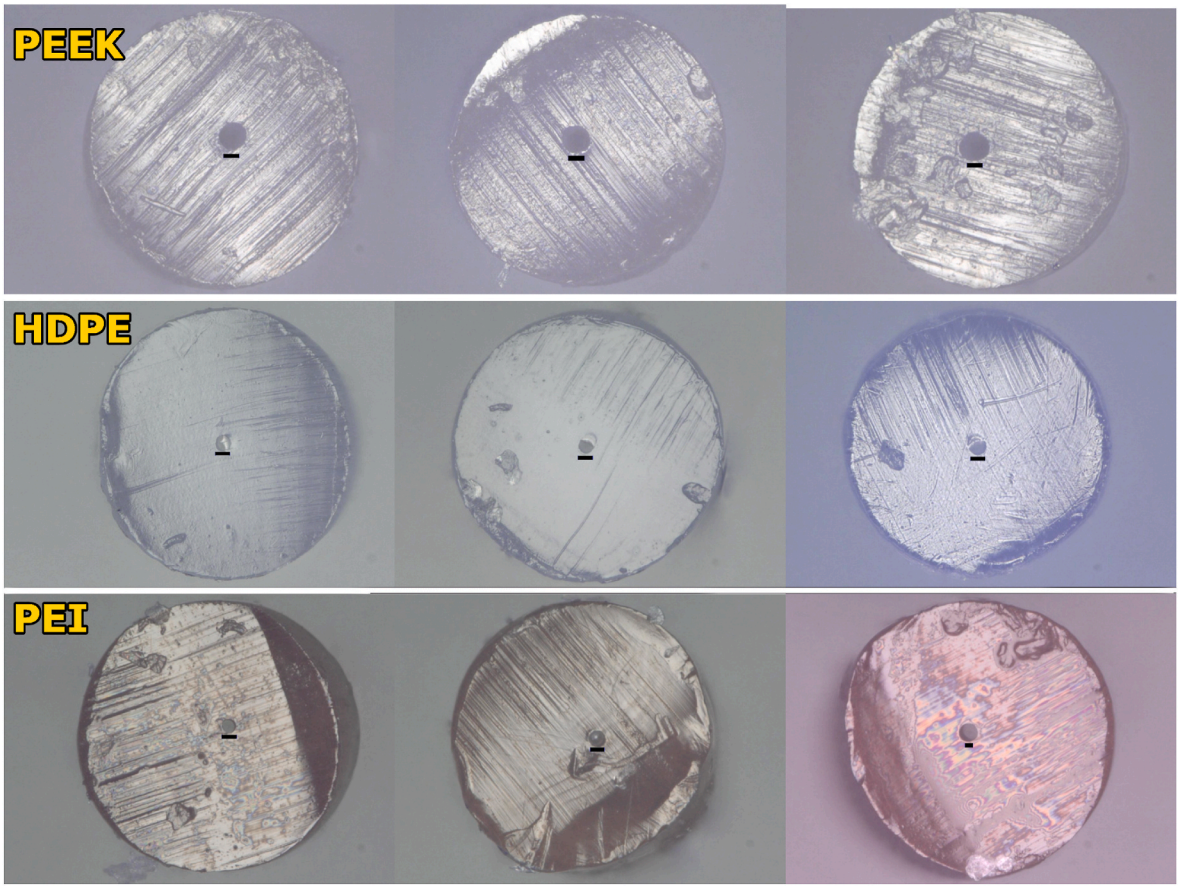

Fig. 3. Uniformity of bore. These cross sections were randomly taken from different capillary strands but from the same batch. For the photomicrographs shown, the mean (±SD) φ were 37 (±1), 21 (±1), and 23 ± 4 µm for PEEK, HDPE, and PEI capillaries, respectively. For reference, manufacturer-specified or target extrusion φ values were 25, 20, and 25 µm, respectively. The scale bar is 10 µm in only the right bottom pane; all others are 20 µm.

5.2. Volume measurement results

5.2.1. Gravimetry

Using a fill-liquid of greater density will provide a greater weight difference, and hence better resolution in determining the average diameter. From this standpoint, mercury would be the best fill liquid. However, surface tension of mercury on any of the present polymeric surfaces is so high that it is very difficult to prevent the mercury from

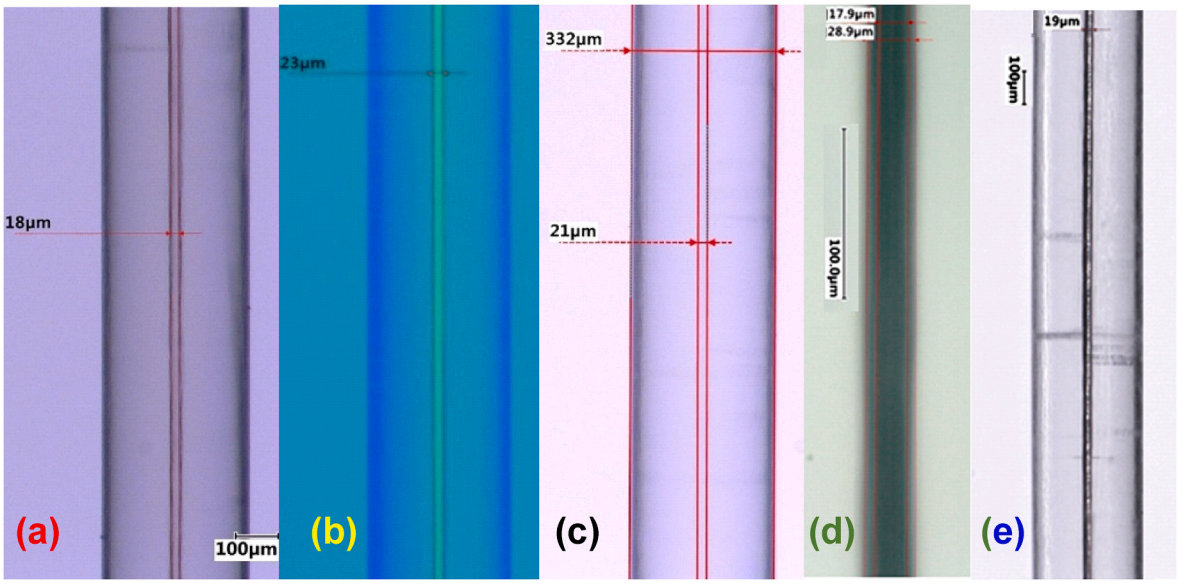

Fig. 4. Transverse photomicrographic image of HDPE capillaries. (a) An air-filled capillary has the highest contrast but this measurement is usually lower than the others (b) A blue light illuminated fluorescein filled capillary, in contrast, always shows slightly higher results than the others. (c) A methylene blue filled capillary. With so little optical depth the dye cannot actually be seen, a water-filled capillary produces the same φ of 21 μm within experimental error. (d) and (e) show a mercury-filled capillary in transmitted and reflected light, respectively. In (d) either the inner or the outer edge can be used; one underestimates and the other overestimates the true φ. The mean, median, and standard deviation of the 21 results (none can be rejected at the 95% confidence level) reported in Table 1 are 21.6, 21.0, and 1.2, respectively. (For interpretation of the references to color in this figure legend, the reader is referred to the Web version of this article.)

Table 1
Diameter of the HDPE capillary measured by various techniques.

φ, μm (%RSD, n)		
Individual Measurements	Via Slope[a] Plot	Results
1. Volume Measurement		
1.1 Gravimetry		
20.2 (2.5, 4)	N/A[b], water-filled	
21.2 (N/A, 1)	N/A, Galinstan filled	
1.2 Dilution Factor		
1.2.1 Conductance		
22.0 (3.7, 8)	C_{dil} vs. length	20.9 (4.9, 4)
1.2.2 Absorbance		
19.1 (0.8, 8)	C_{dil} vs. length	20.1 (3.7, 4)
1.2.3 Fluorescence		
21.6 (1.9, 4)	C_{dil} vs. length	21.4 (1.7, 4)
2. Mercury Conductance		
20.5 (0.5, 6)	Resistance vs. length	20.4 (0.9, 3)
3. Hagen-Poiseuille Relation		
3.1 Constant single pressure, measure flow		
18.9 (1.7, 4)		N/A
18.4 (2.7, 4)		N/A
22.0 (1.3, 3)		N/A
All		
19.6 (8.1, 11)		N/A
3.2 Adjust flow measure pressure		
21.8 (1.3, 4)	Flow vs. Pressure	21.7 (0.9, 4)
22.2 (0.8, 4)	Flow vs. Pressure	22.1 (0.3, 4)
22.0 (1.5, 4)	Flow vs. Pressure	22.0 (0.7, 4)
Composite		Composite
22.0 (1.3, 12)	Flow vs. Pressure	22.0 (0.5, 4)

[a] The reported uncertainty is the uncertainty of the slope of the best fit line, n represents the number of points in the.
[b] Not applicable.

spilling out of the capillary. Determining the position of the meniscus inside the capillary to correct for incomplete filling requires microscopic examination (possible only with transparent/translucent capillaries), and due to lack of adhesion of mercury on any of these polymer surfaces, the mercury column shifts easily. There are several organic liquids that are substantially denser than water (e.g., diiodomethane has a density of 3.3), but most such liquids we tried swell the polymers, thus changing the dimensions, and/or permeate through the walls rather readily.

The internal volume of a 1-m long capillary of 20 μm φ is ~300 nL, resulting in a weight difference of 0.3 mg between an empty and a water-filled capillary. With a balance of 0.015 mg reproducibility, it would be difficult to achieve a precision better than ~5%; much longer tube lengths may improve precision but are increasingly cumbersome to fill. As the calculation of φ involves taking the square root of the actual measurand (equations (4) and (5)) the precision improves by a factor of 2. This was observed in practice. For 4 individual HDPE capillaries ranging from 96.0 to 100.0 cm in length, the weight of the water was 0.0032 ± 0.0001 mg/cm (Av ± SD; 4.4% RSD) and the corresponding φ values were 20.2 ± 0.5 μm (2.5%) RSD. The precision of measuring the same capillary repeatedly by this technique was virtually the same. If the uniformity of the bore were much worse than this precision, the bore variance would have been measurable by this technique by measuring different segments, but this would not be possible if the bore variance was comparable or less than the measurement precision. The latter appears to be the case for HDPE capillaries. While this method is very simple and requires only commonly available equipment, it will be increasingly imprecise, however, as the diameter decreases further. For a balance with 15 μg "reproducibility" (we interpret this as the ±2 SD span or 4 SD), the limit of quantitation will be 10 SD or 38 μg. With a 1-m tube length and water as the fill liquid, 7 μm φ will thus be the smallest capillary that can be measured by this approach. This can improve significantly if a heavier fluid (e.g., Galinstan, density 6.4) is used instead of water.

Filling with Galinstan was tried with two 1.0 m lengths of a PEI and a single length of HDPE capillary. Unlike mercury, no self-expulsion difficulty was encountered. The density value for Galinstan determined with the benchmark silica capillary of known diameter was within 3% of the literature value. The gravimetrically determined φ for the HDPE capillary was 21.2 μm, in good agreement with that measured with water as the fill liquid (20.2 ± 0.5 μm). That for the PEI-01 and PEI-02 capillaries were 20.9 and 25.6 μm, respectively; however, recall that photomicrographic measurements indicated that the PEI capillaries have a relatively large variance in bore.

Fig. 5. Effect of fluid refractive index on the optically perceived diameter in transverse imaging. The manufacturer stated and cross section measurement optical diameter was 25.2 ± 0.2 μm.

5.3. Dilution factor measurements

Compared to gravimetric measurement with water as the fill liquid, much greater measurement span is possible in the dilution factor approach using purely aqueous fill liquids, regardless of which sub-approach below is used. Here, there are essentially three parameters that dictate the attainable measurement span: (a) the maximum possible concentration (C_{known}, eq (5)) of the original solution taken for dilution (multimolar for suitable highly conductive electrolytes, and ≳ 100 mM for many strongly absorbing/fluorescing dyes (e.g., methylene blue in water, fluorescein in strong alkali): (b) the minimum volume of the diluted solution that can be conveniently measured (we take this to be 5 mL, as standard 1 cm path optical cuvettes have a volume of 3 mL; certainly, <1 mL will be inconvenient); and finally (c) the lowest concentration of the diluted solution (C_{dil}, eq (5)) that can be accurately quantitated (C_{LOQ}). The maximum dilution factor attainable, DF_{max}, is thus

$$DF_{max} = C_{known}/C_{LOQ} \quad (9)$$

whereas the actual dilution factor, DF_{act} is given by

$$DF_{act} = V_{dil}/V \quad (10)$$

these terms having been previously defined in reference to eq (5).

5.3.1. Via conductance

Compared to the other options, DF_{max} can be somewhat lower in conductance measurements because C_{LOQ} is higher. This is not because of any intrinsic insensitivity of conductance measurements but due to variations in CO_2 contamination of the sample which creates a variation in the background conductance. Under conditions in which a constant low background can be maintained and conductance is measured under well-thermostated conditions, as in suppressed hydroxide eluent ion chromatography, changes in conductance less than 1 nS/cm can be detected. Presently, without conducting all experiments in a CO_2-free glovebox, a specific conductance level ≲ 1 μS/cm (corresponding to ca. 6.7 μM KCl in the absence of CO_2 contamination) cannot be accurately related to any added electrolyte concentration. For 6–48 μM KCl, the conductance calibration plot was linear with an r^2 of 0.9989, a slope of 0.143 μS/(cm.μM), close to the theoretical value of 0.149 μS/(cm.μM) and an intercept of 0.51 μS/cm, possibly due to intrusion of CO_2. The C_{dil} values for 25, 50, 75, and 100 cm tubes were 10.5 ± 0.4, 21.8 ± 0.8, 30.6 ± 1.4, and 36.6 ± 1.2 μM, representing an r^2 of 0.98 but with a significant intercept of 3 μM. The average (±SD) φ value from all 8 measurements was 22.0 ± 0.8 μm: this rsd of 3.7% was indistinguishable from the mean 3.4 ± 1.0% rsd of the diameters computed for each individual tube. The bore uniformity of the tubes therefore cannot be assessed from these data.

Although we used a C_{known} of ~1 M, slightly more than 3 M is possible for KCl. DF_{max} is therefore ~4.5×10^5. The choice of KCl was dictated by its routine use as a conductance standard and its facile availability in pure form. Certain other electrolytes may permit a higher DF_{max}; H_2SO_4, for example, is substantially more concentrated and has a much greater specific conductance in dilute solution. Concentrated H_2SO_4 (~18 M) may be difficult because of its hygroscopic nature and high viscosity but 50% H_2SO_4 (~18 eq/L) should be viable; in this case an LOQ of 1 μS/cm equates to a concentration of 2.5×10^{-6} eq/L, resulting in a DF_{max} of 7.2×10^6.

5.3.2. Via absorbance

For flow-through HPLC detectors, typical absorbance LODs are ~5×10^{-6} absorbance units (AU). Even for modest benchtop spectrometers using static cuvette measurements, LOQs are ~3×10^{-4}AU or better (much better performance is possible with only minor modifications [31]). For a dye with a molar absorptivity of 10^5 this translates to an LOQ of 3×10^{-9} M. For a maximum value of C_{known} conservatively being 0.1 M, DF_{max} will be 3×10^7. And again, this value is conservative: very substantial gains in LOD are possible using a liquid core waveguide cell [32] or other approaches.

Methylene blue was first considered but because of its tendency to adsorb on surfaces, we chose bromothymol blue with $C_{known} = 67.1$ mM. The acidic form of the dye has a substantially lower molar absorptivity (~2×10^4) than the base form, but it is immune to CO_2 intrusion. The same tubes used in the conductance measurements were used. The average of 8 measurements provided a φ of 19.1 ± 0.8 μm, an RSD of 4.5%, indistinguishable from the mean precision of 4.0 ± 0.8% obtained at each tube length.

5.3.3. Via fluorescence

The calibration for fluorescein in the 0.23–3.73 μM range was linear (r^2 0.9998). The average diameter calculated from the replicate measurement of the four tube lengths was 21.4 ± 0.4 μm (1.7% RSD), essentially the same as the precision of replicate measurements (1.1 ± 0.9%). This measurement also did not allow us to conclude about the bore uniformity of the tubes; on the other hand, the fluorescence approach allowed a more precise measurement than the other two alternatives at the 95% significance level. The experimental DF was in the range of 2.8×10^4–1.1×10^5 whereas maximum C_{known} being ≥0.1 M and the LOQ on this particular spectrometer being ~1 nM, DF_{max} was ≳ 10^8. Compared to the two other DF measurement approaches, superior S/N in the fluorescence measurements is likely the reason for better

precision.

5.4. Electrical resistance measurement

There are slight variations in the reported specific resistance of mercury (9.57–9.80 × 10^{-5} Ω cm, see Refs. [33–35]); there is also a compilation of resistivity values of mercury obtained in different experiments [36], albeit dated. We were also uncertain of the purity of the mercury at hand. For this reason, the system was calibrated with various lengths of a fused silica capillary of known diameter (specified to have a beginning i.d. of 25.0 μm and an ending i.d. of 25.3 μm in a 250-m spool). The resistance values of 5 different lengths (19.0–98.7 cm) of mercury filled silica capillaries ranged from 368.7 to 1920 Ω. A plot of the observed resistance vs the length exhibited a highly linear correlation (r^2 = 0.9990) with a slope of 19.42 ± 0.34 Ω/cm and an intercept statistically indistinguishable from zero. If the true diameter is assumed to be 25.15 μm, the specific resistance ψ for mercury would be calculated to be 9.64 ± 0.17 × 10^{-5} Ω cm, very much in the middle of the reported values for the metal.

The resistance of three lengths (30.0, 48.0, and 90.0 cm) of mercury-filled HDPE capillaries were similarly measured to be 879.0, 1382, and 2871 Ω. Using the ψ value determined above, the respective φ values were computed to be 20.46, 20.64, and 20.47 μm, in excellent agreement with each other. Obviously, the resistance exhibited an excellent linear relationship with length (r^2 = 0.9998) and a slope of 29.40 ± 0.38 Ω/cm, from which φ would be calculated to be 20.43 μm with an RSD of 0.89%. In measurement precision, this method outshines all the others tried and would be the method of choice were it not for the hazards posed by mercury.

Galinstan offers a superior alternative from toxicity aspects. The ψ value, at 2.89 × 10^{-5} Ω cm @ 20 °C [37] is somewhat higher than mercury but this still leads to resistance values that are easily and accurately measurable by most instruments. Although the viscosity of Galinstan is ~50% greater than that of mercury, it was not problematic to introduce into various capillaries we tried – Galinstan wets most surfaces; as such, surface tension was not a factor in the pressure necessary for introduction of Galinstan into a capillary, quite unlike mercury. Calibration with a silica capillary of known diameter as with mercury gave the ψ value to be 2.90 × 10^{-5} Ω cm, essentially no different from the literature value. Galinstan is nontoxic, making it unquestionably preferred over mercury. Although it is more expensive than mercury, the amount used is minuscule.

There is one caveat about the electrical contact used for resistance measurement with Galinstan. It attacks most metals, dissolving/alloying them or getting into the lattice. Because one paper reported there is no effect on stainless steel on prolonged contact and even in the presence of high levels of electrical current [38], we attempted to use a small SS reservoir within and in contact with the larger SS pressure chamber. The smaller vial was used in case SS is attacked, the larger reservoir will not be contaminated. The other end used a Pt -wire electrode. Resistance readings were unstable and dependent on probe polarity; further investigation showed that a net potential is present across the two electrodes; stainless steel is not totally inert to Galinstan. When Pt contacts were used on both sides, resistance could be measured without problems. Graphite contacts/containers could presumably be used as well.

The resistance-based measurement of the PEI-01 and PEI-02 capillaries indicated respective φ values of 20.4 and 22.3 μm.

5.5. Hagen-Poiseuille relationship

5.5.1. Single fixed pressure measure flow

Diameters obtained for HDPE-01 through HDPE-03 were 18.91 ± 0.32 (n = 4), 18.45 ± 0.49 (n = 4), and 21.97 ± 0.30 (n = 3) μm. While the first two results were not distinguishable from each other, the third was different from the other two at the 95% probability level.

PEI-03, PEI-04, and PEI-05 respectively measured 21.9, 22.6, and 22.0 μm by this approach.

5.5.2. Change flow measure pressure

The same three HDPE capillaries measured 21.8 ± 0.3, 22.2 ± 0.2, and 22.0 ± 0.1 μm (n = 4 ea.) based on individual measurements at the four flow rates. There was no particular trend of the determined diameter with the flow rate used. When calculated from the slope of the flow vs pressure plots, the φ for HDPE-01 through HDPE-03 were 21.7 ± 0.2, 22.1 ± 0.1, and 22.0 ± 0.1_5 μm, respectively. These values were individually indistinguishable from the average individual measurements above and also from each other. It is interesting to note that φ for HDPE-03 as measured in sec. 5.5.1 is also indistinguishable from these results but the results for HDPE-01 and HDPE-02 are different at the 95% confidence level. These experiments were conducted at room temperature without thermostating. However, temperature variation that we have observed in our laboratory (±1.5 °C), cannot alone account for the observed difference (viscosity varies 2%/°C, but the effect of that is greatly attenuated due to the 4th root dependence of φ on viscosity (eq. (8)). We believe that the difference may have been caused by overtightening of the compression fitting connecting the tube.

5.6. Assessment of uniformity of φ from measurements that have different dependence on φ

While diameters may not be obtained accurately by transverse observation of the bore for transparent/translucent capillaries, an assessment of bore uniformity may still be possible. Beyond transparency limitations, the high magnification needed to observe such small inner diameters with sufficient acuity greatly restricts the field of view. As such, scanning the bore diameter over any significant length can both be tedious and take an inordinate amount of time. Cutting a capillary every *x* cm and examination of the cross section may provide a measure of the variance of φ, but it destroys the capillary and hardly provides an assurance that this variance would apply to the next length of capillary used, especially when the variance is high.

It occurred to us that while the different measurement techniques each produces a weighted average value over the length of the capillary, the different techniques *do not average in the same manner*. Any measurement that is dependent fundamentally on the value of the cross section (e.g., volume or resistance), averages r^2, for example. In contrast, measurements relying on the Hagen-Poiseuille equation will produce a value that averages r^4. These values will be equal only if the variance is zero. If measurements are sufficiently precise relative to the variance, this difference in radius obtained by two appropriately different techniques can provide both the true value of *r* and its variance.

As a simple example, consider a capillary consisting of two segments, one with a radius of $r + a$, the other with a radius of $r - a$, the average being *r*. when the average of the squares (r^2_{av}) is taken, this would be

$$r^2_{av} = \tfrac{1}{2}\left((r+a)^2 + (r-a)^2\right) = r^2 + a^2 \tag{11}$$

Conversely, if r^4 was being averaged, one would calculate for the same capillary

$$r^4_{av} = \tfrac{1}{2}\left((r+a)^4 + (r-a)^4\right) = r^4 + 6r^2a^2 + a^4 \tag{12}$$

If *r* and *a* were 10.00 and 5.00 μm, respectively, volume measurement techniques will suggest a radius of 11.18 μm while pressure drop measurements would suggest 12.65 μm, both of which overestimates the actual radius. The degree of discrepancy between the two measurements increases with an increase in the variance and this in turn would increase the magnitude of the overestimation. This is illustrated in Fig. 6. Conversely, from two disparate measurements that depend differently on how φ is averaged, both the actual diameter and its variance can be computed. Of course, a real situation does not consist of tubes that have just two segments of unequal diameters – it would be customary to

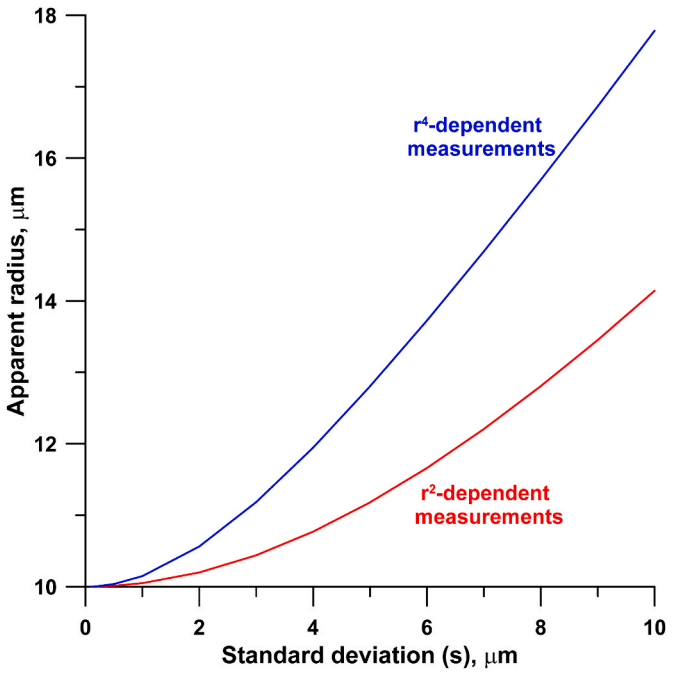

Fig. 6. The figure shows the apparent radii that will be measured for a capillary tube with an inner radius *r* of 10 μm and radius variance that follows a normal distribution with a standard deviation (s) as noted in the abscissa. The Poiseuille-dependent measurements (red trace) rely on averaging r^4, while all the other measurements described in this paper average r^2. (For interpretation of the references to color in this figure legend, the reader is referred to the Web version of this article.)

assume that φ would follow a continuum with a normal distribution.

It can be shown (see supporting information for the derivation) that for a tube of radius *r* whose radius follows a normal distribution with a standard deviation of *s,* the applicable version of the expression for r^2_{av} is not very different from eq (11):

$$r^2{}_{av} \cong r^2 + s^2 \tag{13}$$

However, the expression for r^4_{av} becomes a bit different:

$$r^4{}_{av} \cong r^4 + 6r^2s^2 + 3s^4 \tag{14}$$

Algebraic manipulation of eqs (13) and (14) (See SI for derivation) yields

$$r = \sqrt[4]{\frac{3\left(r^2_{av}\right)^2 - r^4_{av}}{2}} \tag{15}$$

Whence *s* can be calculated from eq (13).

The PEI capillaries seemed to show the largest variance and would therefore be amenable to such treatment. The apparent diameters of three separate segments of PEI capillaries, each 0.98–0.99 m in length, were measured by the Galinstan-filled conductometry and the Pressure-flow behavior (Hagen-Poiseuille equation) in triplicate, with utmost care to ensure reproducibility. The results for the calculated values of the true φ and its standard deviation, shown in Table 2, are consistent with each other and with other data presented on this capillary in the foregoing.

Table 2
Conductometric and Poiseuille diameters measured for PEI capillaries.

PEI tube #	Galinstan-filled conductometric φ, μm	Water flow Poiseuille φ, μm	Calculated true φ, μm	Calculated standard deviation s, μm
1	21.9 ± 0.0	22.0 ± 0.0	21.8 ± 0.0	1.8 ± 0.0
2	22.6 ± 0.0	23.3 ± 0.0	22.2 ± 0.0	4.1 ± 0.0
3	22.0 ± 0.0	22.8 ± 0.0	21.6 ± 0.0	2.1 ± 0.0

6. Consequence of bore variance in OTLC

Studies of the consequences of column bore variation in chromatography are scant. Recently Gritti et al. [39] have theoretically examined the behavior of a packed column that is conically shaped with the inlet φ being 4.2 mm and the exit φ being 2.1 mm, especially during gradient elution. In comparison with a column of uniform 3 mm φ, the efficiency decreases somewhat (albeit not dramatically) and performs worse if the smaller end is made the inlet. The authors point out nevertheless that in ultrafast gradient separations, conical columns may have some advantages for certain analytes. It is implicitly recognized in OTLC that at a fixed flow rate that the plate height H decreases and thence separation efficiency increases as the column bore φ decreases. Much earlier, Giddings [40] theoretically examined the behavior of columns of nonuniform bore in capillary gas chromatography and concluded that the efficiency inevitably decreases compared to a column of uniform bore when the results are compared for the same retention time for a particular analyte in the two cases. Much of this effect arises from the compressibility of gases. Although Giddings argues in the appendix of this work that a similar effect would be true for incompressible fluids as well, in OTLC the rate of diffusive mass transfer is often the determining factor in governing efficiency. Indeed, according to the Gormley-Kennedy equation [41], mass transfer to the walls of a tube at a *fixed volumetric flow rate* is *independent* of the diameter of a tube. The consequences of variation of the bore uniformity in OTLC have never been examined, theoretically or experimentally. In a single column, the flow rate is the same throughout the column so when the bore cross section varies, the flow velocity changes in a reciprocal fashion. As separations are typically carried out at eluent velocities greater than the optimum to save time, while a locally increased bore will reduce the local efficiency, the concomitant decrease in flow velocity may ameliorate the deleterious effect of an increased bore to a degree. In any case, the effects of bore variation along the length of a single capillary must be different from the capillary-to-capillary bore variation in a parallel multicapillary bundle, in that case, at the same head pressure, an increased diameter would result in a lower flow resistance and larger flow rate. For a single capillary, rather than relying on the Gormley-Kennedy equation, which assumes that analyte sticking coefficient to the wall is unity, we can consider the situation from the kinetic perspective of traditional chromatographic theory.

Knox and Gilbert [42] simplified the Golay equation for open tubular gas chromatography for OTLC in terms of the reduced plate height *h* (*h* = H/φ, H being the plate height) and the reduced velocity *υ* (*υ* = *u*φ/*D*, where u is the eluent velocity and *D* the diffusion coefficient of the analyte in the eluent):

$$h = \frac{2}{\upsilon} + \frac{1 + 6\,k\, +\, 11\,k^2}{96(1+k)^2}\,\upsilon \tag{16}$$

where *k* is the retention factor for the analyte. In a simpler form one can express this as:

$$h = \frac{2}{\upsilon} + x\upsilon \tag{17}$$

where *x* has values between 0.01 and 0.1 (0.0104, 0.0147, 0.01910, 0.0312_5, 0.0469, 0.0660, 0.0885, and 0.0999 for k = 0, 0.1, 0.2, 0.5, 1, 2, 5, and 10, respectively). Noting that $H = \varphi h$, and that the volumetric flow rate *F* is given by

$$F = \pi u \varphi^2/4 = \pi \upsilon D \varphi/4 \tag{18}$$

The plate height *H* would be given by

$$H = \frac{\pi D\varphi^2}{2F} + \frac{4xF}{\pi D} = \frac{(\pi D\varphi)^2 + 8\,xF^2}{2\pi DF} \tag{19}$$

If we are considering the plate counts N for a length L, N would then be given by

$$N = L \Big/ H = \frac{2\pi DFL}{(\pi D\varphi)^2 + 8\,xF^2} \tag{20}$$

As a control, a plot of eq (20) for three different values of φ and without any bore variation is shown in Figure S2. The reciprocal of the plate counts are shown in Figure S3 as the traditional Van Deemter plot; Figure S4 shows the plate heights in a logarithmic scale to better depict the minimum.

Next, to simulate the effect of diametric variation on plate counts, we assumed that a column consists of many sequential elements of different diameters where the diameter frequency distribution follows a Gaussian pattern. Five cases were assumed for a column of $\varphi_{mean} = 20$ μm, with the standard deviation s being 0, 1, 2, 3, and 4 μm respectively. In each case, we considered the distribution of φ over a Z-range [43] of ± 3.5, which encompasses 99.95% of the population. The cumulative probability values corresponding to these Z-scores were then generated, e.g., by the NORMDIST function in Excel with a resolution of $\Delta Z = 0.01$–0.04 for $s = 1$, 2, 3, and 4 μm, respectively. Each of these Z values correspond to $\varphi = \varphi_{mean} + Zs$. The difference between two successive probability values then gives the relative frequency of occurrence of a diameter that is the average of these two successive φ values. We take this probability slice to be the length of the column that has this diameter. Eq. (20) was then used to compute the plate counts for each individual element at various flow rates ranging from 0.01 to 5 nL/s for k values ranging from 0 to 10 (an illustrative spreadsheet is given as a SI file.) In each case the plate counts for all the individual length elements of the column were summed to determine the total plate count. The results are shown in Fig. 7.

It will be observed that there is practically no effect of the breadth of the diameter distribution on the column efficiency, as would be expected if the system exhibits Gormley-Kennedy behavior. Only a minute departure is observed for very low values of k and at very low flow velocities, the difference from the perfectly uniform case increasing with increasing diameter variance. Even then, for $k = 0$ (a case where Gormley-Kennedy behavior will not be expected) the maximum difference is ≲ 2%. The odd part of the behavior in the minimum plate height region is that one would intuitively expect a uniform diameter to provide the best performance, but that is not the case. One surmises that the better efficiency of the smaller diameter half slightly outweighs the worse performance of the larger diameter half. In any case, the effect is marginal, happens at too low eluent flow rates and only for very low k analytes to be of practical interest. The reassuring aspect is that the poorer bore uniformities of polymer capillaries do not make them inherently inferior for chromatographic use.

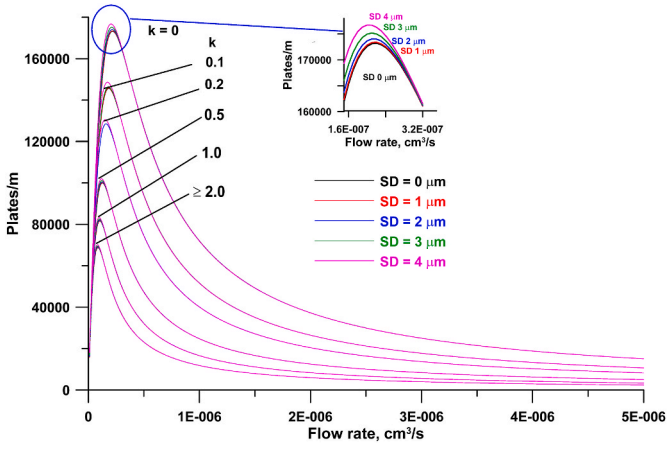

Fig. 7. Predicted efficiencies of a capillary of 20 μm mean i.d. with standard deviations of 0, 1, 2, 3, and 4 μm, for analytes of retention factors (k) ranging from 0 to 10, as a function of eluent flow rates of 0.01–5 nL/s (0.6–300 nL/min, nominally 0.03–16 mm/s) for an analyte with a diffusion coefficient of 10^{-5} cm^2/s. Note that any effect of bore nonuniformity can only be seen at very low k values and low velocities. The Van Deemter optimum flow rate shows a minor shift to lower flow rates with increasing bore nonuniformity.

7. Conclusions

While silica capillaries are by far the most commonly used and typically display ideal geometry, polymer capillaries can be attractive in some applications for mechanical, chemical and cost reasons. Geometric characterization is important as manufacturing technology is immature and manufacturer specifications (if available), can be grossly inaccurate. Circularity, concentricity and bore uniformity are all important parameters but only circularity has a defined quantitative index. We define herein such a concentricity index for the first time. The other, perhaps the most important parameter, is the inner diameter. While photomicrography of the cross section can provide this measurement, nondestructive measurement of bore uniformity has been tedious to impossible. Although transverse imaging is possible for translucent/transparent capillaries, an accurate value is difficult to obtain. Methods that measure the diameter in an integrated manner include those that give a measure of the square of the i.d. φ (such as via measuring the contained volume, or by measuring the electrical resistance of a liquid metal filled capillary) and those that give a measure of φ^4 (such as those that measure the pressure required to achieve a certain flow rate through the tube, or the obverse). We show that when φ has significant variance, both the φ^2 and especially the φ^4 dependent measurements will provide values greater than the true values. But if both are measured, it is possible to get both the true φ value and its variance. Of integrated φ measurement methods, gravimetric methods using a water-filled capillary is the simplest but in the absence of a microbalance, the lower end measuring capabilities are limited. The latter is improved if much denser Galinstan or any other such room temperature liquid metal/alloy is used as the fill liquid. Electrical resistance measurement with a liquid metal filled capillary provides the most precise results. However, Galinstan sticks to the capillary inner surface and removing the same by acid dissolution is slow. For capillaries with reasonably uniform bore, all of the methods tried produce results that are very close. Finally, the effect of bore variance of performance on separation efficiency in open tubular liquid chromatography was theoretically studied. While not experimentally verified yet, as long as the mean i.d. remains the same, theory predicted no effects of diameter variance (even substantial) on the separation efficiency, as long as the mean diameter remains constant.

CrediT authorship contribution statement

PKD conceived and directed the work and wrote the final manuscript, EY carried out most of the experimental work and provided the first draft of the manuscript, including some of the graphics and trained SAH who picked up when EY left for maternity and carried out remaining experiments, CPS provided day to day help and supervision in the lab and assisted in preparing the final version of the manuscript; SR contributed to the mathematical aspects, especially the derivation of eqs (13) and (14).

Consent for publication

Written informed consent for publication was obtained from all participants.

Declaration of competing interest

The authors declare that they have no known competing financial interests or personal relationships that could have appeared to influence the work reported in this paper.

Data availability

Data will be made available on request.

Acknowledgment

This work was supported by NASA grant 80NSSC19K0805 through the MatISSE program, the National Science Foundation grant CHE-2003324, Thermo Fisher Scientific and the Hamish Small Chair endowment. We thank Dr. Miroslav Dohnal for his many efforts towards making near-perfect HDPE capillaries in a small enough diameter regime.

Appendix A. Supplementary data

Supplementary data to this article can be found online at https://doi.org/10.1016/j.aca.2022.340345.

References

[1] D.H. Desty, J.N. Haresnape, B.H.F. Whyman, Construction of long lengths of coiled glass capillary, Anal. Chem. 32 (1960) 303–304, https://doi.org/10.1021/ac60158a057.
[2] G. Nota, G. Marino, V. Buonocor, A. Ballio, Liquid-solid chromatography with open glass capillary columns. Separation of 1-dimethylaminonaphthalene-5-sulphonyl amino acids, J. Chromatogr. 46 (1970) 103–106, https://doi.org/10.1016/S0021-9673(00)83969-2.
[3] R.D. Dandeneau, E.H. Zerenner, An investigation for glasses for capillary chromatography, J. High Resolut. Chromatogr. 2 (1979) 351–356, https://doi.org/10.1002/jhrc.1240020617.
[4] X. Huang, C. Horváth, Capillary zone electrophoresis with fluid-impervious polymer tubing inside a fused-silica capillary, J. Chromatogr. A 788 (1997) 155–164, https://doi.org/10.1016/S0021-9673(97)00709-7.
[5] W.R. Dean, The stream line motion of fluid in a curved pipe, Philos. Mag. A 5 (1928) 674–695.
[6] W.R. Dean, Note on the motion of fluid in a curved pipe, Philos. Mag. A 4 (1927) 208–223, https://doi.org/10.1112/S0025579300001947.
[7] P.K. Dasgupta, Linear and helical flow in a perfluorosulfonate membrane of annular geometry as a continuous cation exchanger, Anal. Chem. 56 (1984) 96–103, https://doi.org/10.1021/ac00265a027.
[8] P. Moulin, J.C. Rouch, C. Serra, M.J. Clifton, P. Aptel, Mass transfer improvement by secondary flows: dean vortices in coiled tubular membranes, J. Membr. Sci. 114 (1996) 235–244, https://doi.org/10.1016/0376-7388(95)00323-1.
[9] D. Ishii, T. Takeuchi, Study of the performance of cation-exchange columns in open-tubular microcapillary liquid chromatography, J. Chromatogr. 218 (1981) 189–197, https://doi.org/10.1016/S0021-9673(00)82055-5.
[10] A.L. Crego, J.C. Diez-Masa, M.V. Dabrio, Preparation of open tubular columns for reversed-phase high-performance liquid chromatography, Anal. Chem. 65 (1993) 1615–1621, https://doi.org/10.1021/ac00059a022.
[11] A. Manz, W. Simon, Picoliter cell volume potentiometric detector for open tubular column LC, J. Chromatogr. Sci. 21 (1983) 326–330, https://doi.org/10.1093/chromsci/21.7.326.
[12] S.R. Muller, W. Simon, H.M. Widmer, K. Grolimund, G. Schomburg, Separation of cations by open-tubular column liquid chromatography, Anal. Chem. 61 (1989) 2747–2750, https://doi.org/10.1021/ac00199a013.
[13] S.R. Muller, D. Scheidegger, C. Haber, W. Simon, Fast separations with open tubular ion exchange capillary columns, J. High Resolut. Chromatogr. 14 (1991) 174–177, https://doi.org/10.1002/jhrc.1240140307.
[14] W. Huang, A. Plistil, S. Stearns, P.K. Dasgupta, Gradient nanopump based suppressed ion chromatography using PEEK open tubular columns, Talanta Open 3 (2021). Art. 100029. 11 pp, https://doi:10.1016/j.talo.2020.100029.
[15] D. Pyo, P.K. Dasgupta, L.S. Yengoyan, High temperature open tubular capillary column ion chromatography, Anal. Sci. 13 (Suppl) (1997) 185–190, https://doi.org/10.2116/analsci.13.Supplement_185.
[16] X. Huang, C. Horváth, Capillary zone electrophoresis with fluid-impervious polymer tubing inside a fused-silica capillary, J. Chromatogr. A 788 (1997) 155–164, https://doi.org/10.1016/S0021-9673(97)00709-7.
[17] P. Kuban, P.K. Dasgupta, C.A. Pohl, Open tubular anion exchange chromatography. controlled layered architecture of stationary phase by successive condensation polymerization, Anal. Chem. 79 (2007) 5462–5467, https://doi.org/10.1021/ac070690q.
[18] Y. Yang, P. Xiang, A. Chen, S. Liu, Liquid chromatographic separation using a 2 μm id open tubular column at elevated temperature, Anal. Chem. 93 (2021) 4361–4364, https://doi.org/10.1021/acs.analchem.1c00296.
[19] P. Xiang, Y. Piliang, Y. Yang, H. Chen, A. Chen, S. Liu, Liquid chromatography using ≤ 5 μm open tubular columns, TrAC, Trends Anal. Chem. 142 (2021), https://doi.org/10.1016/j.trac.2021.116321. Art. 116321.
[20] A. Chen, K.B. Lynch, X. Wang, J.J. Lu, C. Gu, S. Liu, Incorporating high-pressure electroosmotic pump and a nano-flow gradient generator into a miniaturized liquid chromatographic system for peptide analysis, Anal. Chim. Acta 844 (2014) 90–98, https://doi.org/10.1016/j.aca.2014.06.042.
[21] M. Zhang, B.C. Yang, P.K. Dasgupta, Polymethylmethacrylate open tubular ion exchange columns. Nondestructive measurement of very small ion exchange capacities, Anal. Chem. 85 (2013) 7994–8000, https://doi.org/10.1021/ac4018583.
[22] B.C. Yang, M. Zhang, T. Kanyanee, B.N. Stamos, P.K. Dasgupta, An open tubular ion chromatograph, Anal. Chem. 86 (2014) 11,554–11,561, https://doi.org/10.1021/ac503249t.
[23] W. Huang, S. Seetasang, M. Azizi, P.K. Dasgupta, Functionalized cycloolefin polymer capillaries for open tubular ion chromatography, Anal. Chem. 88 (2016) 12,013–12,020, https://doi.org/10.1021/acs.analchem.6b03669.
[24] W. Rasband. Imagej.. https://imagej.nih.gov/ij/plugins/circularity.html.
[25] D.A.V. Medina, N.G.P. Dos Santos, J.S. da Silva Burato, J.V.B. Borsatto, F. M. Lancas, An overview of open tubular liquid chromatography with a focus on the coupling with mass spectrometry for the analysis of small molecules, J. Chromatogr. A 1641 (2021), 461989, https://doi.org/10.1016/j.chroma.2021.461989.
[26] E.J. Guthrie, J.W. Jorgenson, L.A. Knecht, S.G. Bush, Technique for accurate measurement of capillary lengths and diameters, J. Separ. Sci. 6 (1983) 566–567, https://doi.org/10.1002/jhrc.1240061007.
[27] A.C. Short, M.L. Montoya, S.A. Gebb, R.G. Presson Jr., W.W. Wagner Jr., R. L. Capen, Pulmonary capillary diameters and recruitment characteristics in subpleural and interior networks, J. Appl. Physiol. 80 (1996) 1568–1573, https://doi.org/10.1152/jappl.1996.80.5.1568.
[28] D.A. Tata, B.J. Anderson, A new method for the investigation of capillary structure, J. Neurosci. Methods 113 (2002) 199–206, https://doi.org/10.1016/S0165-0270(01)00494-0.
[29] O. Arend, A. Remky, N. Plange, B.J. Martin, A. Harris, Capillary density and retinal diameter measurements and their impact on altered retinal circulation in glaucoma: a digital fluorescein angiographic study, Br. J. Ophthalmol. 86 (2002) 429–433, https://doi.org/10.1136/bjo.86.4.429.
[30] T. Liu, P. Sen, C.J. Kim, Characterization of nontoxic liquid-metal alloy galinstan for applications in microdevices, J. Microelectromech. Syst. 21 (2011) 443–450, https://doi.org/10.1109/JMEMS.2011.2174421.
[31] P.K. Dasgupta, R. Bhawal, Y.-H. Li, Anal. Chem. 86 (2014) 3727–3734, https://doi.org/10.1021/ac404251w.
[32] T. Dallas, P.K. Dasgupta, TrAC, Trends Anal. Chem. 23 (2004) 385–392, https://doi.org/10.1016/S0165-9936(04)00522-9.
[33] The Physics factbook. Resistivity of mercury. https://hypertextbook.com/facts/2006/MarinaGrintsvayg.shtml.
[34] https://www.periodic-table.org/Mercury-electrical-resistivity/.
[35] D.C. Giancoli, Physics, fourth ed., Prentice Hall, 1995. http://hyperphysics.phy-astr.gsu.edu/hbase/Tables/rstiv.html.
[36] https://en.wikisource.org/wiki/1911_Encyclop%C3%A6dia_Britannica/Conduction,_Electric/Solids.
[37] Ch Karcher, V. Kocourek, D. Schulze, Experimental investigations of electromagnetic instabilities of free surfaces in a liquid metal drop, in: International Scientific Colloquium, Modelling for Electromagnetic Processing, 2003, pp. 105–110.
[38] D.K. Sarfo, R.R. Taylor, A.P. O'Mullane, Investigating liquid metal galinstan as a high current carrier and its interaction with collector electrodes, ACS Appl. Elec. Mater. 2 (2020) 2921–2928, https://doi.org/10.1021/acsaelm.0c00551.
[39] F. Gritti, J. Belanger, G. Izzo, W. Leveille, On the performance of conically shaped columns: theory and practice, J. Chromatogr. A 1593 (2019) 34–46, https://doi.org/10.1016/j.chroma.2019.01.055.
[40] J.C. Giddings, Plate height of nonuniform chromatographic columns. Gas compression effects, coupled columns, and analogous systems, Anal. Chem. 35 (1963) 353–356, https://doi.org/10.1021/ac60196a026.
[41] P.G. Gormley, M. Kennedy, Diffusion from a stream flowing through a cylindrical tube, Proc. Roy. Ir. Acad. Sci. Sect. A 52 (1949) 163–169.
[42] J.H. Knox, M.T. Gilbert, Kinetic optimization of straight open-tubular liquid chromatography, J. Chromatogr. A 186 (1979) 405–418, https://doi.org/10.1016/S0021-9673(00)95263-4.
[43] R.C. Sprinthall, Basic Statistical Analysis, Allyn and Bacon, Boston, 2007. Ch 4.b.